AN ANALYSIS OF THE 3D CRITICAL REGION LENGTH IN LONGITUDINALLY VENTILATED TUNNELS DURING FIRE EVENTS

[1, 2]Ayala, Pablo, [2]Amo, Luis, [1, 2]Cantizano Alexis
[1]Institute for Research in Technology, ICAI, Comillas Pontifical University, ES
[2]ICAI School of Engineering, Comillas Pontifical University, ES

DOI 10.3217/978-3-85125-996-4-37 (CC BY-NC 4.0)

ABSTRACT

Computational models are valuable tools for designing fire ventilation systems in tunnels. However, these models can be very complex and computationally expensive. Moreover, smoke behavior depends on many factors, such as tunnel geometry, ventilation velocity, fire intensity, tunnel slope, etc. Hybrid or multiscale models are alternatives that can lower the computational demand and still produce trustworthy results. These models combine regions with different levels of detail: one-dimensional (1D) and three-dimensional (3D). The 1D regions offer simpler results through faster computation, while the 3D region provides greater realism and detail, albeit at the cost of increased computational resources and time. Defining the 3D region is critical and challenging, as it significantly influences the model's accuracy and efficiency. Its length, i.e., critical length, can be determined by employing various criteria, mainly based on relevant parameters such as the hydraulic diameter or the heat release rate (HRR). In this study, the downstream critical length of a fire in a longitudinally ventilated tunnel is analyzed through a numerical study comprising 108 simulations conducted with FDS 6.8.0. The assessment considers the impact of HRR, tunnel cross-sectional area, and ventilation velocity on the critical length. As HRR increases, downstream critical length grows, expanding the simulation domain and computational cost. Similarly, the critical length slightly rises as the cross-sectional area decreases, but further studies needed for quantitative analysis. These conclusions are drawn from defining critical length based on the tunnel's longitudinal temperature gradient. Furthermore, various models are introduced to illustrate the dimensionless relationship between the critical length and HRR, confirming that a linear relationship is not suitable when longitudinal ventilation is present. The dependency of the critical length on ventilation velocity is quite significant, greatly improving the model's fit when taken into account.

Keywords: CFD, Multiscale, Coupled hybrid modeling, Tunnel fire ventilation, FDS, 3D Region

1. INTRODUCTION

According to several studies, smoke inhalation is the primary cause of death in fires, making its study highly relevant in the field of fire safety, particularly in tunnels [1]. Numerous tunnel ventilation studies have been conducted to assess smoke behaviour based on factors such as fire location, wind influence, vehicle blockage effects, or tunnel temperature distribution, among others [2–4]. Additionally, various full-scale tests have been conducted [5–8], but these come with high costs and environmental impacts. As an alternative, reduced-scale tests with ratios of 1/6 to 1/50 have also been used [9]. However, the inability to maintain complete similarity in dimensionless numbers reduces the precision of their results compared to full-scale tests. With technological advancements, Computational Fluid Dynamics (CFD) models for fire simulation have become widespread in the industry, supporting classic prescriptive designs for assessing smoke and flame behaviour [10–12].

One of the main challenges in CFD models with large domains is the high computational cost, limiting the number of simulations for design optimization. Strategies like Design of Experiments (DoE) are employed to predict potential behaviour [13,14]. Particularly in long tunnels, the use of hybrid models or multiscale models for tunnel fires has become more common due to their reduced computational cost [15–18].

The definition of the 3D-CFD region in hybrid or multiscale models is critical, as it affects both model accuracy and computational cost. A larger 3D domain enhances precision but also increases computational cost. Recent studies have explored the critical length for non-ventilated tunnels, quantifying dimensionless relationships between critical length and HRR. They include analyses using dimensionless methods to assess various tunnel phenomena, such as backlayering length, critical velocity [19], or smoke stratification [19, 20].

This work examines the downstream critical length of a fire in a longitudinally ventilated tunnel through a numerical assessment, involving 108 simulations using FDS 6.8.0 [22]. The influence of HRR, cross-sectional tunnel characteristics, and ventilation velocity is evaluated. Additionally, different models are presented to quantify the downstream critical length.

2. THEORETICAL APPROACH – DIMENSIONAL ANALYSIS

In the case of longitudinally ventilated tunnels, the critical length of the tunnel can be evaluated using a dimensionless model [18, 22, 23]. In these studies, the critical length (L_{ds}) generally depends on the HRR ($\dot{Q}$), ambient temperature (T_0), gravity (g), air specific heat capacity (c_p), air density (ρ_0), and tunnel hydraulic diameter ($\overline{H}$). However, in this work, unlike the previous ones, the bulk velocity of longitudinal ventilation is also included. Thus, the downstream critical length of the fire can be expressed as:

$$L_{ds} = f(Q, T_0, g, c_p, \rho_0, \overline{H}, u_0)$$

Thus, we obtain the following relationship of dimensionless groups:

$$\frac{L_{ds}}{\overline{H}} = f\left(\frac{Q}{\rho_0 c_p T_0 \overline{H}^{\frac{5}{2}} g^{\frac{1}{2}}}, \frac{u_0}{(g\overline{H})^{\frac{1}{2}}}\right) = f(Q^*, V^*)$$

For scenarios without ventilation, a linear model between the dimensionless critical length (L^*) and HRR ($Q^{*1/3}$) is proposed by Wang [24]:

$$L^* = 95 Q^{*1/3}$$

In this study, we will analyze the fitting of simulation data with three different models.

Linear model: $L^* = c_1 \, Q^{*1/3}$

Potential model: $L^* = c_1 \left(Q^{*1/3}\right)^{c_2}$

Linear model with velocity dependency: $L^* = c_1 \, Q^{*1/3} + c_2 \ln(c_3 V^*)$

3. CASES OF STUDY

3.1. Numerical models

Different numerical models have been developed in FDS 6.8.0, an open-source software commonly used by the industry. This software employs the Eddy Dissipation Concept (EDC) with a thermal extinction model to simulate combustion. Turbulence is simulated using the Deardorff model (C_v=0.1), and radiation is considered using the radiation transport equation with 100 angles. Additionally, the maximum number of iterations has been set to 100, compared to the default value of 10, defined by FDS, to solve the Poisson equation. This will avoid numerical instabilities due to the extensive domain length of FDS and the high HRR in some cases.

A total of 108 numerical simulations have been conducted to evaluate the influence of various parameters. In Table 1, a summary of the fire scenarios is provided, encompassing scenarios with different HRR and longitudinal ventilation velocities. Furthermore, different cross-sectional areas have been assessed by varying both the width and height of the tunnel.

The tunnel's overall length spans 2,000 meters, with the fire source positioned at 500 m from the upstream portal at a height of 1.2 meters. A HRR per unit area ranging from 1,300 kW/m² to 1,800 kW/m² has been established, adjusted based on the mesh size. The specific configurations are as follows:

- HRR: 5 MW. Fire area: 2.4 x 1.6 m^2
- HRR: 30 MW. Fire area: 6.4 x 3.2 m^2
- HRR: 50 MW. Fire area: 8.8 x 3.2 m^2

Temperature and velocity measurements are conducted at 0.5-meter intervals throughout the entire tunnel, at 0.4 meters from the ceiling, and at a distance of 0.4 meters from the wall.

Table 1: Summary of the values considered for the different parameters

Simulations	HRR (MW)	Velocity (m/s)	Tunnel width (m)	Tunnel height (m)
1-36	5	0 / 1.5 / 3 / 5	6 / 8 / 12	4 / 6 / 8
37-72	30	0 / 1.5 / 3 / 5	6 / 8 / 12	4 / 6 / 8
73-108	50	0 / 1.5 / 3 / 5	6 / 8 / 12	4 / 6 / 8

3.2. Mesh sensitivity analysis

A mesh sensitivity analysis has been conducted with the 8 m wide and 4 m high tunnel model, with 1,000 m length, a longitudinal ventilation velocity of 1.5 m/s and a 5 MW fire centrally positioned. The choice of the mesh size (Δ) has taken into account the characteristic fire diameter (D*) with a spatial resolution analysis $R=D^*/\Delta$, that should be maintained between 1/16 and 1/4 [22]. For this reason, the lowest HRR has been selected since it requires the smallest mesh size. Four mesh sizes have been studied: 0.2 m, 0.2/0.4 m, 0.4 m, and 0.8 m, corresponding to resolutions within the required range. The numerical model with 0.2/0.4 m is divided in such a way that a length of 50 m, centered on the fire, have a mesh size of 0.2 m, and 0.4 m in the rest of the tunnel.

Figure 1 shows the vertical temperature profile and temperature evolution under the ceiling at the centerline of the tunnel, at 20 m (Figure 1a and Figure 1b) and 100 m (Figure 1c and Figure 1d) downstream the fire. At 20 m, vertical temperature profiles exhibit differences between the models. However, these discrepancies decrease as the distance from the fire increases, i.e., being less than 10 ºC at 100 m downstream, which corresponds to an 11% error compared to the finest mesh.

Table 2 shows the relative errors at different downstream locations, with respect to the finest mesh values. It is observed that differences under the ceiling decrease significantly, always staying below 11.2% from 100 m downstream onwards.

Finally, the backlayering length is also influenced by mesh size for the different cases: 18.5 m (0.8 m), 42 m (0.4 m), 44.5 m (0.2/0.4 m), and 49.5 m (0.2 m). It is observed that backlayering length increases as the mesh size becomes smaller, but with differences less than 7 m between the 0.4 m and 0.2 m meshes. These results are similar to those found by McGrattan and Bilson [25], emphasizing how the sensitivity of smoke backlayering length significantly depends on the mesh size and definition criteria applied.

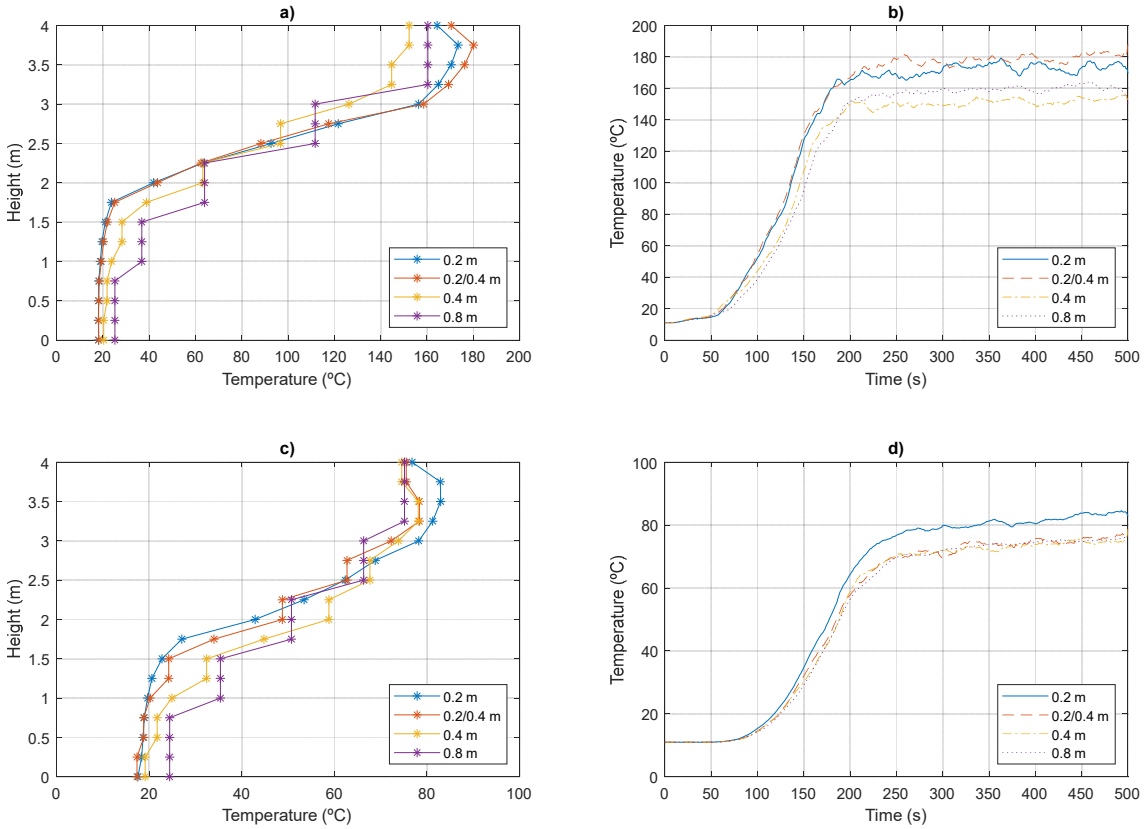

Figure 1: Vertical temperature and temperature evolution under the ceiling in the centerline of the tunnel: at 20 m (a-b) and 100 m downstream the fire (c-d).

Table 2: Relative errors (%) of temperature under the ceiling along the centerline of the tunnel.

Δ (m)	Downstream distance from fire source (m)									
	50	100	150	200	250	300	350	400	450	500
0.2/0.4	6.2	8.9	11.2	10.5	9.9	9.4	8.5	8.9	8.6	8.3
0.4	15.2	10.0	7.4	5.8	3.8	2.6	1.1	1.8	1.9	2.9
0.8	11.7	9.3	8.4	6.2	4.0	2.2	0.9	0.7	1.8	2.2

Based on these results, this study has been conducted with a mesh size of 0.4 m. This mesh configuration not only maintains good accuracy in the distant fire field but also reduces computational costs, requiring only 13.7 hours compared to the 82 hours needed for the simulation with a 0.2 m mesh size. Despite the mesh size not being sufficiently fine for detailed analysis, it is adequate for conducting a qualitative study to analyze the critical length.

3.3. Critical length downstream the fire

Smoke flow characteristics are defined through different regions: near region, one-dimensional flow region, and turbulent mixing region [23,24,26]. These are analyzed based on the temperature distribution along the tunnel. Different methodologies can be found in the literature to define the critical length. This work uses the methodology presented by Wang et al. [24] by calculating a parameter 'k' derived from the temperature difference between two adjacent positions:

$$k = \frac{1}{n}\sum_{i=1}^{n}\frac{T(x_1) - T(x_0)}{x_1 - x_0}$$

The number of data points 'n' depends on the region under consideration and 'k' is close to 1 in the turbulent zone. Here, 'k' is estimated by calculating the average thermal gradient every 10 meters.

Figure 2a illustrates the evolution of the mean temperature under steady-state conditions (during the last 100 seconds of simulation). In Figure 2b, the profile of the 'k' parameter is depicted. This is computed as the average temperature gradient every 0.5 meters over a 10-meter tunnel section. Finally, the critical length is calculated as the position where a 1ºC variation, for every 10 meters of the tunnel, equivalent to a 'k' value of 0.1, as can be seen in the figure with a red mark.

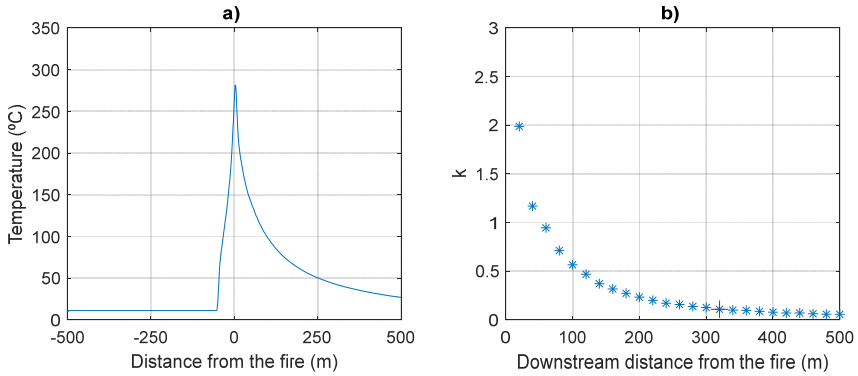

Figure 2: a) Temperature distribution along the centerline of the tunnel; b) k distribution.

4. RESULTS

4.1. HRR and tunnel cross-sectional area influence

The influence of the HRR and the tunnel cross-sectional area on the critical length for different longitudinal ventilation conditions can be observed in Figure 3. Firstly, the influence of the HRR is significant, regardless of the tunnel's cross-sectional area and ventilation. As the HRR rises, the critical length also increases. Nevertheless, the increase in critical length does not correlate proportionally with the rise in HRR. Notably, the disparity within the rise 5-30 MW is significantly larger than in the rise 30-50 MW, particularly at velocities up to 3 m/s. In unventilated scenarios, the average difference of critical lengths for rise 5-30 MW amounts to 330 m, whereas it is only 20 m for rise 30-50 MW. At a ventilation rate of 1.5 m/s, the average difference for both 5-30 MW and 30-50 MW, remains substantial (330 m and 85 m, respectively). This trend persists at 3 m/s, where the average difference for rise 5-30 MW is 490 m, contrasting with 160 m for rise 30-50 MW. Lastly, the average increments at 5 m/s are comparable for both rises: 290 m (5-30 MW) versus 260 m (30-50 MW). In summary, the average differences for rise 5-30 MW seem unsignificant at any ventilation speed. However,

for rise 30-50 MW, there is a pronounced dependency on velocity, with differences escalating notably with velocity.

Considering every value of HRR, for a 5 MW fire, it is observed that as the ventilation velocity increases, the critical length decreases. This reduction ranges from an average of 288 m for models without ventilation to 64 m for a ventilation speed of 5 m/s. This could be explained as ventilation facilitates the attainment of uniform temperature conditions over a shorter distance downstream of the fire. In the 30 MW scenario, for ventilation velocities up to 3 m/s, the average values of critical length are approximately 600 m, with a difference of less than 50 m depending on the ventilation rate. However, at 5 m/s velocity, the average critical length reduces to 350 m. Ultimately, the 50 MW scenarios are the least influenced by ventilation velocity, as their average lengths range between 610 and 750 m for any ventilation rate.

Regarding the influence of the tunnel cross-sectional area, despite the inability to draw direct conclusions from the graph, a trend emerges: the critical length slightly increases as the tunnel width decreases, particularly for higher HRR values and lower ventilation speeds. Similarly, for a given width, the critical length slightly decreases as the height increases. However, the differences in critical lengths do not follow a fixed pattern, indicating the need for further analysis to draw more precise conclusions.

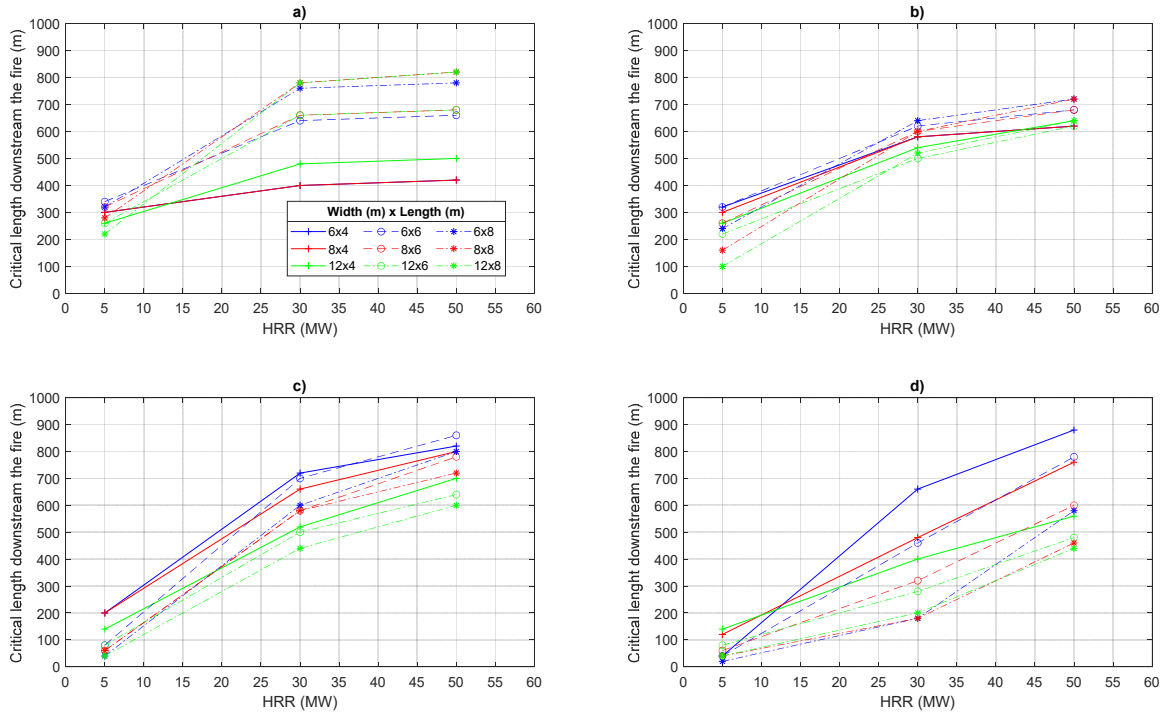

Figure 3: Critical downstream length for different longitudinal velocities: a) 0 m/s, b) 1.5 m/s, c) 3 m/s, and d) 5 m/s.

4.2. Dimensionless model

Figure 4 illustrates various fitting curves between the downstream critical length of the fire and the dimensionless HRR for different scenarios of longitudinal ventilation: 0 m/s, 1.5 m/s, 3 m/s and 5 m/s. In each scenario, simulation data is represented in different colours: 5 MW (blue), 30 MW (red), and 50 MW (green). It is evident that there is a clear relationship between $Q^{*1/3}$ and L^* at low HRR values. As mentioned in the previous section, the data has been fitted to three types of curves: linear, potential, and linear with velocity dependency.

For the scenarios without longitudinal ventilation, the coefficients obtained for linear and potential models are:

Linear	Potential
$L^* = 130\ Q^{*1/3}$	$L^* = 114\ \left(Q^{*1/3}\right)^{0.7}$
$R^2 = 0.85$	$R^2 = 0.82$

Secondly, for the scenario of longitudinal ventilation at 1.5 m/s, Figure 3b includes linear and potential fits as well as linear fit with velocity dependency. In this case, it is observed that the predictions made by all three models are accurate. The coefficients obtained are:

Linear	Potential	Linear with velocity
$L^* = 137\ Q^{*1/3}$	$L^* = 147\ \left(Q^{*1/3}\right)^{1.2}$	$L^* = 155\ Q^{*1/3} + 32 \ln(3.7\ V^*)$
$R^2 = 0.92$	$R^2 = 0.94$	$R^2 = 0.96$

For the scenario of a ventilation velocity of 3 m/s, Figure 3c shows that the potential model fits well and is comparable to that considering velocity. However, the linear fit deviates considerably from the previous ones. The coefficients obtained are:

Linear	Potential	Linear with velocity
$L^* = 145\ Q^{*1/3}$	$L^* = 204\ \left(Q^{*1/3}\right)^{1.9}$	$L^* = 254\ Q^{*1/3} + 3.7 \ln(10^{-8}\ V^*)$
$R^2 = 0.78$	$R^2 = 0.96$	$R^2 = 0.97$

Finally, the results obtained with a longitudinal ventilation of 5 m/s are similar to those obtained for the ones of 3 m/s, as shown in Figure 3d. Similarly, the linear fit is less accurate. The coefficients obtained are:

Linear	Potential	Linear with velocity
$L^* = 112\ Q^{*1/3}$	$L^* = 214\ \left(Q^{*1/3}\right)^{2.9}$	$L^* = 225\ Q^{*1/3} + 40.2 \ln(0.3V^*)$
$R^2 = 0.63$	$R^2 = 0.92$	$R^2 = 0.90$

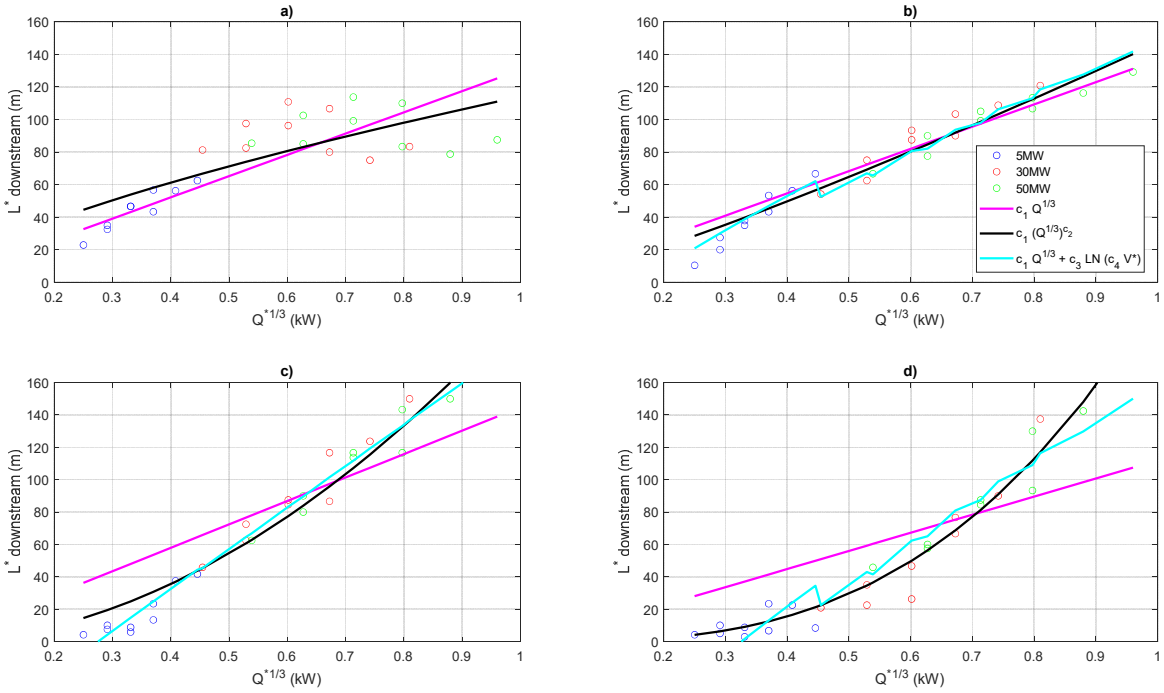

Figure 4: Fitting curves between dimensionless critical length and dimensionless HRR for different ventilation velocities: a) 0 m/s, b) 1.5 m/s, c) 3 m/s, and d) 5 m/s.

5. CONCLUSION

The study presented investigates the downstream critical length of a fire in a tunnel under various ventilation conditions. A total of 108 numerical models are developed, incorporating three different heat release rates (5 MW, 30 MW, and 50 MW), four different ventilation velocities (0 m/s, 1.5 m/s, 3 m/s and 5 m/s), three different widths (6 m, 8 m, 12 m), and three different heights (4 m, 6 m and 8 m). The objective is to assess the influence of HRR and tunnel cross-sectional area on the critical length under different longitudinal ventilation speeds.

It has been observed that a higher HRR leads to an increase in the downstream critical length, resulting in a larger 3D domain, with consequently, higher computational costs. Additionally, the critical length slightly increases as the cross-sectional area decreases. However, for a quantitative analysis, further studies are required. These conclusions are derived from defining the critical length based on the spatial gradient of the tunnel's longitudinal temperature.

Furthermore, adjustments of the data to different fitting models are presented. These models aim to illustrate the dimensionless relationship between the critical length and HRR. It is noted that the linear relationship between HRR and critical length becomes inadequate in the presence of longitudinal ventilation. Notably, the influence of ventilation velocity on the critical length is substantial, significantly enhancing the model's accuracy when appropriately considered.

This study is based on a definition of a critical length through the tunnel's longitudinal temperature gradient, but further analysis on its definition should be studied, for example, through velocity, transverse velocity and temperature distributions, or smoke stratification analysis, among other options, given the vital importance of this parameter in such studies. Additionally, there should be an emphasis on proposing models that allow for the quantification of this critical length under different ventilation conditions.

6. REFERENCES

[1] A review of tunnel fire research from Edinburgh - ScienceDirect, (n.d.). https://www.sciencedirect.com/science/article/abs/pii/S0379711216300273 (accessed January 11, 2024).

[2] L. Yi, D. Luan, L. Yang, T. Chen, H. Tao, Z. Xu, C. Fan, Flow field and fire characteristics inside a tunnel under the influence of canyon cross wind, Tunnelling and Underground Space Technology 105 (2020) 103575. https://doi.org/10.1016/j.tust.2020.103575.

[3] A. Król, M. Król, Numerical investigation on fire accident and evacuation in a urban tunnel for different traffic conditions, Tunnelling and Underground Space Technology 109 (2021) 103751. https://doi.org/10.1016/j.tust.2020.103751.

[4] M. Weng, I. Obadi, F. Wang, F. Liu, C. Liao, Optimal distance between jet fans used to extinguish metropolitan tunnel fires: A case study using fire dynamic simulator modeling, Tunnelling and Underground Space Technology 95 (2020) 103116. https://doi.org/10.1016/j.tust.2019.103116.

[5] Memorial Tunnel Fire Ventilation Test Program. Interactive CD-ROM and Comprehensive Test Report, Massachusetts Highway Department, 1996., (n.d.).

[6] A. Haack, Fire protection in traffic tunnels: General aspects and results of the EUREKA project, Tunnelling and Underground Space Technology 13 (1998) 377–381. https://doi.org/10.1016/S0886-7798(98)00080-7.

[7] T. Yan, S. MingHeng, G. YanFeng, H. JiaPeng, Full-scale experimental study on smoke flow in natural ventilation road tunnel fires with shafts, Tunnelling and Underground Space Technology 24 (2009) 627–633. https://doi.org/10.1016/j.tust.2009.06.001.

[8] Runehamar tunnel fire tests - ScienceDirect, (n.d.). https://www.sciencedirect.com/science/article/abs/pii/S0379711214001660 (accessed February 28, 2020).

[9] P. Lin, Y.-Y. Xiong, C. Zuo, J.-K. Shi, Verification of Similarity of Scaling Laws in Tunnel Fires with Natural Ventilation, Fire Technol 57 (2021) 1611–1635. https://doi.org/10.1007/s10694-020-01084-9.

[10] W. Wang, Z. Zhu, Z. Jiao, H. Mi, Q. Wang, Characteristics of fire and smoke in the natural gas cabin of urban underground utility tunnels based on CFD simulations, Tunnelling and Underground Space Technology 109 (2021) 103748. https://doi.org/10.1016/j.tust.2020.103748.

[11] A. Cantizano, P. Ayala, E. Arenas, J.R. Pérez, C. Gutiérrez-Montes, Numerical and experimental investigation on the effect of heat release rate in the evolution of fire whirls, Case Studies in Thermal Engineering (2022) 102513. https://doi.org/10.1016/j.csite.2022.102513.

[12] P. Ayala, A. Cantizano, G. Rein, C. Gutiérrez-Montes, Factors affecting the make-up air and their influence on the dynamics of atrium fires, Fire Technology 54 (2018) 1067–1091.

[13] P. Ayala, A. Cantizano, E.F. Sánchez-Úbeda, C. Gutiérrez-Montes, The Use of Fractional Factorial Design for Atrium Fires Prediction, Fire Technol 53 (2017) 893–916. https://doi.org/10.1007/s10694-016-0609-z.

[14] M. Król, A. Król, Multi-criteria numerical analysis of factors influencing the efficiency of natural smoke venting of atria, Journal of Wind Engineering and Industrial Aerodynamics 170 (2017) 149–161. https://doi.org/10.1016/j.jweia.2017.08.012.

[15] F. Colella, G. Rein, R. Borchiellini, J.L. Torero, A Novel Multiscale Methodology for Simulating Tunnel Ventilation Flows During Fires, Fire Technology 47 (2011) 221–253. https://doi.org/10.1007/s10694-010-0144-2.

[16] M. Pachera, X. Deckers, T. Beji, Capabilities and Limitations of the Fire Dynamics Simulator in the Simulation of Tunnel Fires with a Multiscale Approach, J. Phys.: Conf. Ser. 1107 (2018) 042016. https://doi.org/10.1088/1742-6596/1107/4/042016.
[17] C. Xu, Y. Li, X. Feng, J. Li, Multi-scale Coupling Analysis of Partial Transverse Ventilation System in an Underground Road Tunnel, Procedia Engineering 211 (2018) 837–843. https://doi.org/10.1016/j.proeng.2017.12.082.
[18] D. Álvarez-Coedo, P. Ayala, A. Cantizano, W. Węgrzyński, A coupled hybrid numerical study of tunnel longitudinal ventilation under fire conditions, Case Studies in Thermal Engineering 36 (2022) 102202. https://doi.org/10.1016/j.csite.2022.102202.
[19] Y.Z. Li, B. Lei, H. Ingason, Study of critical velocity and backlayering length in longitudinally ventilated tunnel fires, Fire Safety Journal 45 (2010) 361–370. https://doi.org/10.1016/j.firesaf.2010.07.003.
[20] J.S. Newman, Experimental evaluation of fire-induced stratification, Combustion and Flame 57 (1984) 33–39. https://doi.org/10.1016/0010-2180(84)90135-4.
[21] H. Nyman, H. Ingason, Temperature stratification in tunnels, Fire Safety Journal 48 (2012) 30–37. https://doi.org/10.1016/j.firesaf.2011.11.002.
[22] K. McGrattan, R. McDermott, S. Hostikka, J. Floyd, FDS (Version 6) user's guide, Technical report, NIST, 2013.
[23] Z. Wang, X. Jiang, H. Park, L. Wang, J. Wang, Numerical Investigation on the length of the near-field region of smoke flow in tunnel fires, Case Studies in Thermal Engineering 28 (2021) 101584. https://doi.org/10.1016/j.csite.2021.101584.
[24] Z. Wang, X. Jiang, F. Tang, J. Li, Study on critical length for simulation in tunnel fires, Tunnelling and Underground Space Technology 115 (2021) 104013. https://doi.org/10.1016/j.tust.2021.104013.
[25] K. McGrattan, M. Bilson, Modeling longitudinal ventilation in tunnels using fire dynamics simulator, Fire Safety Journal 141 (2023) 103982. https://doi.org/10.1016/j.firesaf.2023.103982.
[26] J. Ji, F. Guo, Z. Gao, J. Zhu, J. Sun, Numerical investigation on the effect of ambient pressure on smoke movement and temperature distribution in tunnel fires, Applied Thermal Engineering 118 (2017) 663–669. https://doi.org/10.1016/j.applthermaleng.2017.03.026.